Targeted inhibition of the extracellular signal-regulated kinase kinase pathway with AZD6244 (ARRY-142886) in the treatment of hepatocellular carcinoma

Hung Huynh,[1] Khee Chee Soo,[2] Pierce K.H. Chow,[3] and Evelyn Tran[1]

[1]Laboratory of Molecular Endocrinology, Division of Cellular and Molecular Research, National Cancer Centre and Departments of [2]General Surgery and [3]Experimental Surgery, Singapore General Hospital, Singapore, Singapore

Abstract

Hepatocellular carcinoma (HCC) is a common malignancy in Asia and Africa. We previously reported that overexpression of extracellular signal-regulated kinase (ERK) kinase 1/2 (MEK1/2) and ERK1/2 was detected in HCC, and that their activation was required for liver cancer cell proliferation and survival. In the present study, we determined the efficacy of a specific MEK1/2 inhibitor AZD6244 (ARRAY-142886) in treatment of HCC. Treatment of primary HCC cells with AZD6244 led to growth inhibition, elevation of the cleavage of caspase-3 and caspase-7, and cleaved poly(ADP)ribose polymerase, but inhibition of ERK1/2 and p90RSK phosphorylation. Studying the protein expression profile of seven HCC xenografts revealed that their growth rate was positively correlated with the levels of phosphorylated MEK. AZD6244, when given p.o. to mice bearing these xenografts, resulted in a dose-dependent inhibition of tumor growth. AZD6244-induced growth suppression was associated with inactivation of ERK1/2 and p90RSK, and up-regulation of activated caspase-3 and caspase-7, and cleaved poly(ADP)ribose polymerase. Our data suggest that the MEK-ERK pathway plays an important role in the growth and survival of liver cancer cells and that the HCC xenograft models are excellent tools for screening preclinical drugs. Targeted inhibition of the MEK-ERK pathway with AZD6244 may represent an alternative approach for the treatment of this disease. [Mol Cancer Ther 2007;6(1):138–46]

Received 7/26/06; revised 10/11/06; accepted 11/17/06.

Grant support: Singapore Cancer Syndicate grant SCS-AS32 (H. Huynh).

The costs of publication of this article were defrayed in part by the payment of page charges. This article must therefore be hereby marked *advertisement* in accordance with 18 U.S.C. Section 1734 solely to indicate this fact.

Requests for reprints: Hung Huynh, Laboratory of Molecular Endocrinology, Division of Cellular and Molecular Research, National Cancer Centre of Singapore, Singapore 169610, Singapore. Phone: 65-436-8347; Fax: 65-226-5694. E-mail: cmrhth@nccs.com.sg

doi:10.1158/1535-7163.MCT-06-0436

Introduction

Hepatocellular carcinoma (HCC) is the fifth most common cancer worldwide (1). The incidence is ~626,000 new cases per year in 2002 (2). The disease is associated with environmental exposure to hepatitis B and C viruses, and aflatoxin B1 (3, 4). It is frequently seen as both a unifocal as well as a multifocal disease. Patients with poorly differentiated tumors or cirrhosis in their tumor sample exhibit poorer survival (5). Treatment outcomes for HCC have remained poor. The majority of patients with HCC have inoperable disease with very poor prognosis (6). In general, the majority of patients die within 12 months of diagnosis. The 5-year survival rate is only 25% to 39% after surgery (7–9). Long-term survival is uncommon because of frequent recurrence, metastasis, or the development of new primaries (10, 11). Moreover, there is no currently accepted adjuvant or palliative treatment modalities that have been conclusively shown to prolong survival (12).

Several lines of evidence indicate that HCC might be the result of a combination of the inactivation of tumor-suppressor genes, activation of multiple oncogenes, and overexpression of growth factors (13). More than 20 cellular genes have been associated with HCC (13, 14). One of the most frequent targets downstream of receptor and non–receptor tyrosine kinases and the ras family of GTP-binding proteins is the extracellular signal-regulated kinase (ERK) kinase (MEK)-ERK signal transduction pathway. This pathway is involved in proliferation, differentiation, apoptosis, and angiogenesis (15). It is constitutively active in a variety of solid tumor models, including lung, colon, pancreas, and breast (15). Elevated levels of constitutively activated MEK1 are frequently seen in carcinoma cell lines (16, 17). Studies with small-molecule inhibitors of MEK activity (18) have shown a role for MEK in mediating cell motility (19) and the expression of protein kinases implicated in invasion and metastasis (20, 21). No substrates of MEK have been identified other than p44/42 ERK1/2 (22). Treatment of cells with various growth factors produces activation of MEK1/2 and its downstream target, ERK1/2, resulting in proliferation, differentiation, and survival (23). Activation of the MEK-ERK pathway regulates the activity of a number of substrates through phosphorylation (24). The 90,000 daltons ribosomal S6 kinases (RSK1–RSK3), a family of broadly expressed serine/threonine kinases, is also activated by ERK1/2 in response to many growth factors, polypeptide hormones, and neurotransmitters (25).

We previously showed that phosphorylation of MEK1/2 was detectable by immunohistochemistry in 100% (46 of 46) of the HCCs examined. Overexpression and phosphorylation of ERK1/2 was also detected in 91% (42 of 46) and 69% (32 of 46) of the HCCs studied, respectively (26). *In vitro*,

treatment of human HepG2 and Hep3B cells with the MEK1/2-specific inhibitor U0126 led to growth inhibition and apoptosis. Overexpression of activated MEK1 in HepG2 resulted in up-regulation of cyclin D1 and an increase in growth rate (27). Thus, MEK1/2 represents an excellent target for pharmacologic intervention in HCC.

The benzimidazole ARRY-142886 (AZD6244) has been reported to be highly potent MEK inhibitor, with an IC_{50} of 12 nmol/L against purified MEK (15). AZD6244 is an oral, non-ATP competitive inhibitor and highly specific for MEK1/2, a key enzyme in the Ras-Raf-MEK-ERK pathway. AZD6244 had minimal effects on the p38, c-Jun-NH_2-kinase, phosphatidylinositol 3-kinase, and MEK5/ERK5 pathways (28). AZD6244 inhibits both basal and induced levels of ERK1/2 phosphorylation in numerous cancer cell lines with an IC_{50} as low as 8 nmol/L. It has also shown efficacy in numerous tumor models (29). Sustained inhibition of ERK activity in tumors can be achieved at a dose of 10 mg/kg/d in xenograft studies in mice (28). AZD6244 is currently in phase I clinical trials.

In this study, we show that treatment of primary HCC cells with AZD6244 leads to a time- and dose-dependent reduction in cell proliferation and apoptosis. P.o. delivery of AZD6244 to mice bearing HCC xenografts resulted in dose-dependent growth suppression. The data suggest that blocking MEK-ERK activity with AZD6244 may represent a novel approach to the treatment of HCC.

Materials and Methods

Reagents

AZD6244 (AstraZeneca, Macclesfield, United Kingdom) was dissolved in DMSO to a final concentration of 20 mmol/L and stored frozen under light-protected conditions at −20°C. Antibodies against cleaved caspase-7 (20 kDa), cleaved caspase-3, phosphorylated MEK1/2 at $Ser^{217/221}$, phosphorylated MEK1 (Thr^{286}), phosphorylated ERK1/2 at $Thr^{202/Tyr204}$, p90RSK, phosphorylated p90RSK at $Ser^{359/363}$, phosphorylated p90RSK at Ser^{380}, phosphorylated p90RSK at $SerThr^{573}$, and cleaved poly(ADP)ribose polymerase (PARP; 89 kDa) were obtained from Cell Signaling Technology (Beverly, MA). Anti–B-Raf antibody, myelin basic protein (MBP), and recombinant ERK-1 were from Upstate (Charlottesville, VA). Anti–phosphorylated MEK1 ($Ser^{218/222}$) antibody was from Epitomics, Inc. (Burlingame, CA). Antibodies against MEK1, ERK1, and α-tubulin were from Santa Cruz Biotechnology, Inc. (Santa Cruz, CA). Conjugated secondary antibodies were supplied by Pierce (Rockford, IL). The chemiluminescent detection system was supplied by Amersham Pharmacia Biotech (Arlington Heights, IL). Tissue culture dishes and eight-chamber slides were from Lab-Tek Chamber Slide System, Nunc, Inc. (Naperville, IL). The Cell Proliferation ELISA (bromodeoxyuridine) and *In situ* Cell Death Detection kits were obtained from Roche Diagnostics Corporation (Indianapolis, IN).

HCC Xenografts

The study received ethics board approval at the National Cancer Centre of Singapore as well as the Singapore General Hospital. All mice were maintained according to the ''Policy on Humane Care and Use of Laboratory Animals'' published by the NIH. The animals were provided with sterilized food and water *ad libitum*, and housed in negative pressure isolators with 12 h light/dark cycles.

Xenografts were carried out with mice homozygous for the *SCID* (severe combined immunodeficiency) mutation (*SCID/SCID*; The Jackson Laboratory, Bar Harbor, ME). Tumors were minced under sterile conditions and fragments that passed through an 18-gauge needle were mixed with RPMI 1640 for transplantation in *SCID* mice. Seven of eight primary HCCs developed into xenografts. The creation and characterization of these lines of xenografts were previously reported (30).

To investigate the effects of AZD6244 on HCC xenografts, AZD6244 was suspended in water at an appropriate concentration. Mice bearing HCC xenografts were p.o. given, twice a day, with either 100 μL of water ($n = 12$) or 50 mg ($n = 12$) or 100 mg ($n = 12$) of AZD6244 per kilogram of body weight for 21 days, starting from day 7 after tumor implantation. Growth of established tumor xenografts was monitored at least twice weekly by Vernier caliper measurement of the length (a) and width (b) of the tumor. Tumor volume was calculated as $(a \times b^2)/2$. Animals were sacrificed 3 h after the last dose of ADZ6244, and body and tumor weights were recorded, with the tumors harvested for analysis.

To study the effects of AZD6244 on caspase-3 activation and MEK1/2 phosphorylation, mice bearing HCC tumors (~800 mm^3) were treated with vehicle ($n = 4$) or 50 mg of AZD6244 per kilogram of body weight ($n = 4$) for 3 days as described above. Animals were sacrificed 3 h after the last dose, and tumors were harvested and frozen in liquid nitrogen for later analysis. Part of the tumor harvest was fixed in neutral buffer containing 10% formalin for immunohistochemistry.

Immunohistochemical Analysis and Assessment

For immunohistochemical analysis of cleaved caspase-3 and Ki-67, 5-μm sections were cut, dewaxed, rehydrated, and subjected to antigen retrieval as described (14). After blocking endogenous peroxidase activity and reducing nonspecific background staining, the sections were incubated with the primary antibody against cleaved caspase-3 or Ki-67 (overnight at 4°C). Immunohistochemistry was done using the streptavidin-biotin peroxidase complex method, according to the manufacturer's instructions (Lab Vision, Fremont, CA) using 3,3′-diaminobenzidine as the chromogen. Sections known to stain positively were incubated in each batch and negative controls were also prepared by replacing the primary antibody with preimmune sera. For Ki-67, only nuclear immunoreactivity was considered positive. The labeling index was obtained by counting the number of positive cells among 500 cells. They were expressed as percentage values.

Isolation of Primary HCC Cells

Primary cells from 26-1004, 2-1318, and 4-1318 tumors were isolated separately. The tumors were minced and

washed thrice with modified Eagle's medium (MEM). The minced tissue was incubated with MEM containing 5% fetal bovine serum and 5 mg/mL of collagenase (Roche Diagnostics Corporation, Indianapolis, IN) at 37°C for 12 h as described previously (31). Cells were harvested by centrifugation at 800 × *g* for 10 min. The cell pellets were washed thrice with serum-free medium and allowed to grow in growth medium (MEM containing 10% fetal bovine serum).

Cell Viability and Cell Proliferation

Primary HCC cells were plated at a density of 2.0×10^4 per well in growth medium. After 48 h in growth medium, the cell monolayer was rinsed twice with MEM. Cells were treated with various concentrations of AZD6244 (0, 0.5, 1.0, 2.0, 3.0, and 4.0 μmol/L) for 24 or 48 h. Cell viability was determined by the 3-(4,5-dimethylthiazol-2y1)-2,5-diphenyltetrazolium bromide (MTT) assay (32). Cell proliferation was assayed using a bromodeoxyuridine kit (Roche) as described by the manufacturer. Experiments were repeated at least thrice, and the data were expressed as mean ± SE.

Detection of Apoptosis

Primary HCC cells were grown in eight-chamber slides and treated with 0, 0.5, 1.0, 2.0, 3.0, and 4.0 μmol/L of AZD6244 in SRF medium for 24 h. Cells were fixed with PBS containing 4% formalin solution for 1 h at room temperature and washed with PBS. Apoptosis was detected by the terminal deoxynucleotidyl transferase–mediated dUTP nick-end labeling (TUNEL) assay using the *In situ* Cell Death Detection kit (Roche) as described by the manufacturer. Apoptotic cells were then visualized under a fluorescent microscope equipped with a FITC filter. The labeling index was obtained by counting the number of positive cells among 500 cells per region. They were expressed as percentage values.

Western Blot Analysis

Tissue or cells were lysed and subjected to Western blot analysis as previously described (14). Blots were incubated with indicated primary antibodies and 1:7,500 horseradish peroxidase–conjugated secondary antibodies. All primary antibodies were used at a final concentration of 1 μg/mL. The blots were then visualized with a chemiluminescent detection system (Amersham Pharmacia Biotech) as described by the manufacturer.

Assay of MEK Kinase Activity

Anti-MEK1 antibody (Santa Cruz Biotechnology) was used to immunoprecipitate MEK1 molecules. MEK kinase activity was measured as the ability of immuno-isolated MEK1 to activate recombinant ERK1 in a coupled assay using MBP as the end point of the assay (33). Phosphorylated MBP was resolved on a 14% SDS-PAGE gel and vacuum-dried before exposure to X-ray film.

Statistical Analysis

For quantitative analysis, the sum of the density of bands corresponding to protein blotting with the antibody under study was calculated and normalized to the amount of α-tubulin. After normalization with α-tubulin, changes in the expression of the protein under study in the treated samples were expressed relative to the basal levels of this protein in the control sample. Differences in cell number and levels of protein under study were analyzed by ANOVA.

Results

To study the effects of AZD6244 on proliferation and viability, primary HCC cells were studied *in vitro*. For the time course and dose-response experiments, primary 2-1318 cells were treated with vehicle and escalating doses of AZD6244 for 24 and 48 h. Cell viability and cell growth were assessed by MTT assay and bromodeoxyuridine incorporation, respectively. AZD6244 caused a time- and dose-dependent reduction in DNA synthesis (Fig. 1A) and cell viability ($P < 0.01$; Fig. 1B). Significant inhibition of bromodeoxyuridine incorporation was observed as early as 24 h posttreatment ($P < 0.01$). A 50% reduction in cell viability was seen at a dose of <0.5 μmol/L after 48-h incubation (Fig. 1B). Similar results were obtained when 4-1318 and 26-1004 cells were used.

To investigate whether AZD6244-induced growth arrest and apoptosis in primary HCC cells were associated with the inactivation of ERK, lysates from AZD6244-treated 2-1318 cells were subjected to Western blot analysis. AZD6244 treatment caused a dose-dependent elevation of phosphorylated MEK1/2 at $Ser^{217/221}$ and MEK1 at $Ser^{218/222}$; it also caused a loss of ERK1/2 phosphorylation (Fig. 1C). Because MEK phosphorylation is mediated by B-Raf (34), the level of B-Raf was determined. Figure 1C shows that B-Raf expression was increased and was in concordance with MEK phosphorylation. Phosphorylation of p90RSK at $Ser^{359/363}$ was also inhibited by AZD6244, indicating that ERK kinase activity was inactivated (Fig. 1C). We next investigated whether the apoptosis machinery was activated by AZD6244 treatment. As shown in Fig. 1C, the 89-kDa cleaved PARP fragment was detected in the AZD6244-treated samples. The cleaved forms of caspase-3 were readily detectable at a dose as low as 0.5 μmol/L AZD6244 (Fig. 1C). A cleaved caspase-7 fragment was also observed in concordance with caspase-3 activation (Fig. 1C). Figure 1D shows that the rate of apoptosis in primary 2-1318 cells was significantly increased in a dose-dependent manner by AZD6244 ($P < 0.01$). Similar results were obtained when 4-1318 and 26-1004 cells were used.

To study the time course of ERK1/2 and p90RSK inactivation and caspase activation, primary 2-1318 cells were treated with 1 μmol/L of AZD6244 and then harvested at different times for Western blot analysis. As shown in Fig. 2A, phosphorylated ERK1/2 was significantly decreased at 3 h and barely detectable at 6 h after AZD6244 exposure. Phosphorylation of p90RSK was significantly inhibited at 6 h (Fig. 2A). Cleaved forms of caspase-3, caspase-7, and PARP (Fig. 2A) were clearly detected 6 h after AZD6244 treatment and reached maximum levels at 12 h. Inhibition of caspase activation with Z-VAD-FMK completely blocked AZD6244-induced ERK1/2 activation

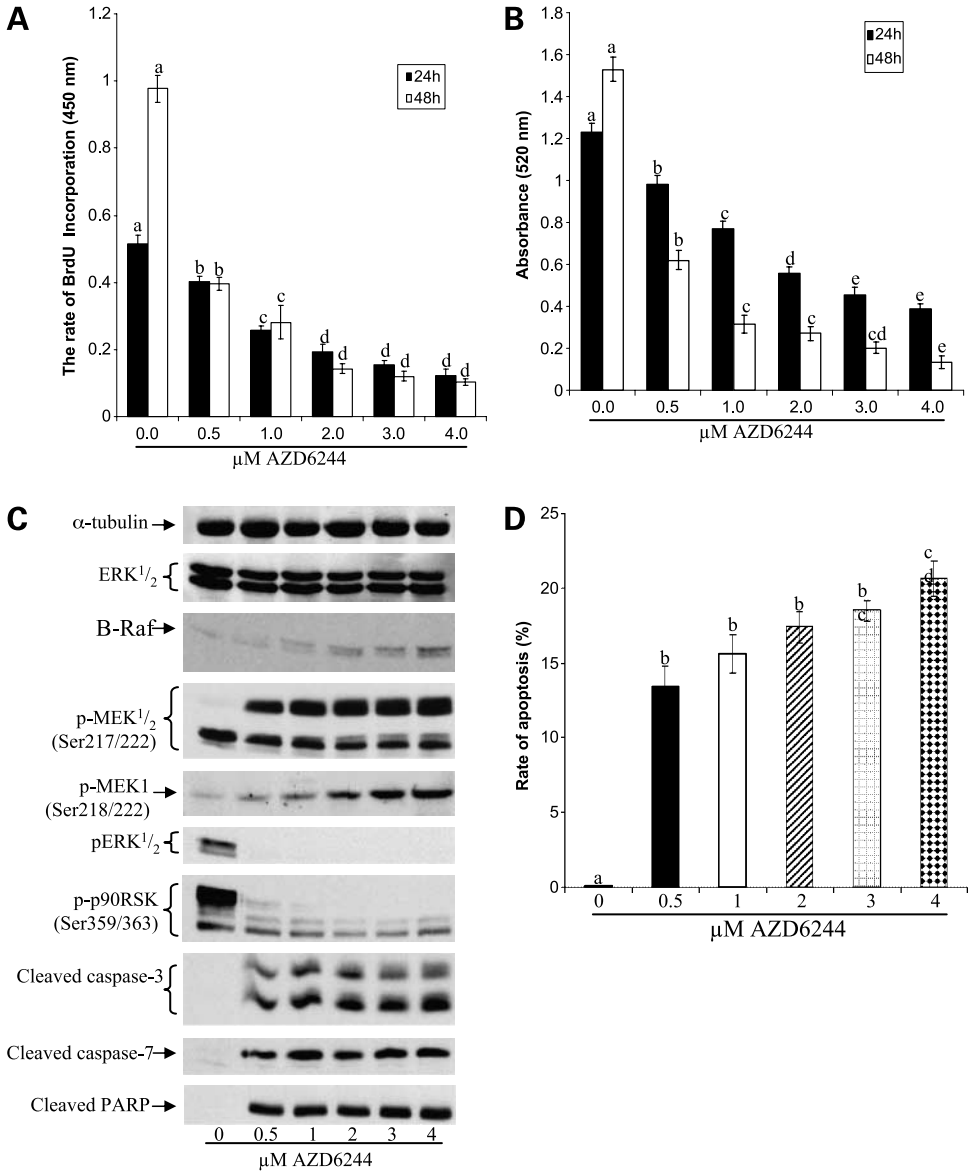

Figure 1. Effects of AZD6244 on cell viability; proliferation; phosphorylation of MEK, ERK1/2, and p90RSK; and apoptosis in primary 2-1318 cells. Primary cells from 2-1318 tumors were isolated as described in Materials and Methods. They were grown and treated with 0.1% DMSO or escalating doses of AZD6244 in serum-free MEM. Cell proliferation and cell viability were determined by bromodeoxyuridine incorporation and MTT assay, respectively, as described in Materials and Methods. Cell proliferation (**A**) and cell viability (**B**) at 24 and 48 h. Experiments were done in quadruplicate. *Columns,* mean; *bars,* SE. **C,** Western blot analysis was done as described in Materials and Methods with cells treated as described above. Blots were incubated with the indicated antibodies and representative samples were shown. **D,** apoptotic cells were determined by TUNEL assay; the rate of apoptosis was expressed as a percentage of the total cells counted. Similar results were obtained when 26-1004 and 4-1318 cells were used. Columns with different letters are significantly different from one another ($P < 0.01$) as determined by ANOVA. *Columns,* mean; *bars,* SE.

and apoptosis in these cells (Fig. 2B), confirming that AZD6244 induced apoptosis in primary 2-1318 cells by activating the caspase pathway.

We previously showed that phosphorylation of MEK1/2 was detectable by immunohistochemistry in 46 of 46 HCCs examined (26), and that activation of MEK-ERK is required for growth and survival of primary HCC cells. To examine the role of MEK-ERK in HCC growth and survival *in vivo*, we established seven (2-1318, 4-1318, 5-1318, 26-1004, 30-1004, 29-1104, and 2006) HCC xenografts from primary HCC tumors. The establishment and characterization of these xenografts are reported elsewhere (30). To investigate whether the difference in growth rate among the different xenograft lines (Fig. 3A) was associated with activation of MEK1/2, Western blot analysis was done. As shown in Fig. 3B, high basal levels of Cdk-5 and phosphorylated MEK1 at $Ser^{218/222}$ and Thr^{286} were detected in the 4-1318 (*lane 5*), 2-1318 (*lane 7*), and 26-1004 (*lane 6*) lines; on the other hand, low basal levels were detected in the 5-1318 (*lane 1*), 29-1104 (*lane 2*), 30-1004 (*lane 4*), and 2006 (*lane 3*) lines. Unexpectedly, the basal levels of phosphorylated ERK1/2 (Fig. 3B) and phosphorylated MEK kinase activity (Fig. 3C), as determined by levels of phosphorylated MBP, in the 2-1318, 4-1318, and 26-1004 lines were slightly lower than those observed in the 5-1318, 29-1104, 30-1004, and 2006 lines. Total ERK1/2 and MEK among xenografts were not significantly different among the lines (Fig. 3B). Thus, the level of phosphorylated ERK1/2 was not in accordance with that of phosphorylated MEK1/2.

To examine the role of MEK in the regulation of HCC growth *in vivo*, mice bearing xenografts that express high (4-1318, 2-1318, and 26-1004) and low (5-1318 and 29-1104)

levels of phosphorylated MEK1 were treated with the MEK inhibitor AZD6244. Both animal toxicity and the ability of AZD6244 to inhibit tumor formation and progression were determined. For the dose-response experiment, 4-1318 xenografts were implanted on both sides of male *SCID* mice. Although a previous study reported that sustained inhibition of ERK activity in tumors could be achieved at a dose of 10 mg/kg/d (28), we were unable to abolish ERK1/2 phosphorylation at that dose in HCC xenografts (data not shown). Therefore, we selected 50 and 100 mg/kg doses of AZD6244 for our *in vivo* study. Mice bearing the 4-1318 xenografts were given p.o. AZD6244 starting on day 7 after tumor implantation. Tumor formation was 100% in both the control and two AZD6244-treated groups. As shown in Fig. 4A, the growth rate of 4-1318 xenografts was decreased by AZD6244 in a dose-dependent manner ($P < 0.01$). The tumor weight in mice treated with 50 and 100 mg ADZ6244 per kilogram was ~40% and 18% of the controls, respectively (Fig. 4B). At a dose of 100 mg/kg, AZD6244 caused ~10% decrease in body weight, suggesting a serious toxicity. No overt toxicity as measured by weight loss, and morbidity was observed at the dose of 50 mg/kg, suggesting good safety. AZD6244 when given at the dose of 50 mg/kg also significantly suppressed the growth of the 5-1318 (Fig. 4C and D), 2-1318 (Fig. 5A), 26-1004 (Fig. 5B), and 29-1104 (Fig. 5C) xenografts ($P < 0.01$). For a dose of 50 mg/kg AZD6244, the treated versus control ratios for 4-1318, 2-1318, 26-1004, 5-1318, and 29-1104 xenografts were 0.41, 0.50, 0.31, 0.64, and 0.70, respectively. The difference in sensitivity to AZD6244, as determined by the treated versus control ratio, between high (4-1318, 2-1318, and 26-1004) and low (5-1318 and 29-1104) MEK1 phosphorylation lines was significant at $P < 0.05$.

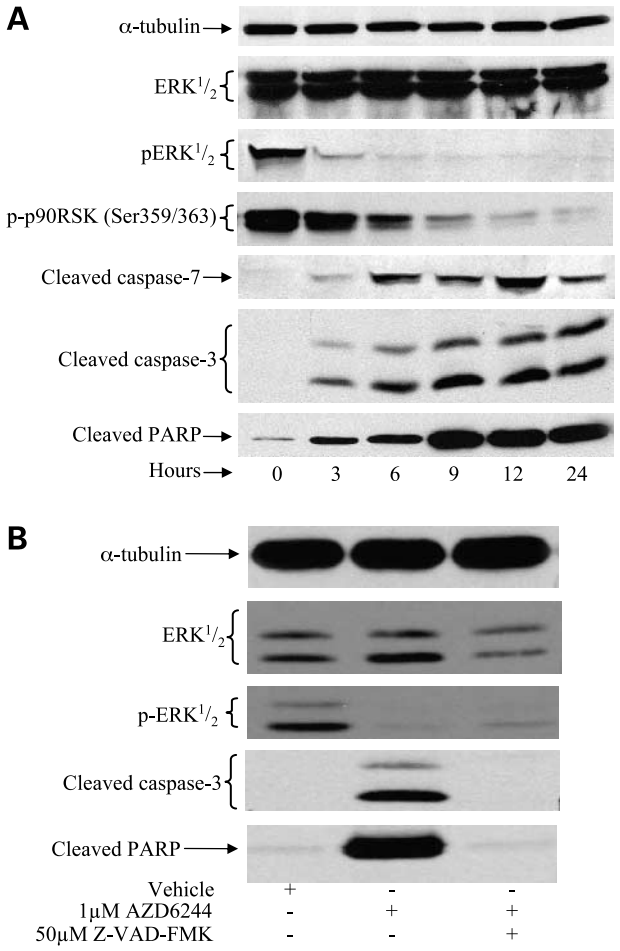

Figure 2. Time-dependent cleavage of caspase-3 and caspase-7 and PARP in primary HCC cells, and caspase-dependent AZD6244-induced apoptosis. Primary HCC cells were isolated and cultured as described in Materials and Methods. **A,** cells were treated with serum-free MEM containing 1 μmol/L AZD6244 for various times. **B,** cells were treated with 1 μmol/L AZD6244 in the presence or absence of 50 μmol/L Z-VAD-FMK for 12 h. Western blot analysis was done as described in Materials and Methods. Blots were incubated with the indicated antibodies. Experiments were repeated thrice with similar results.

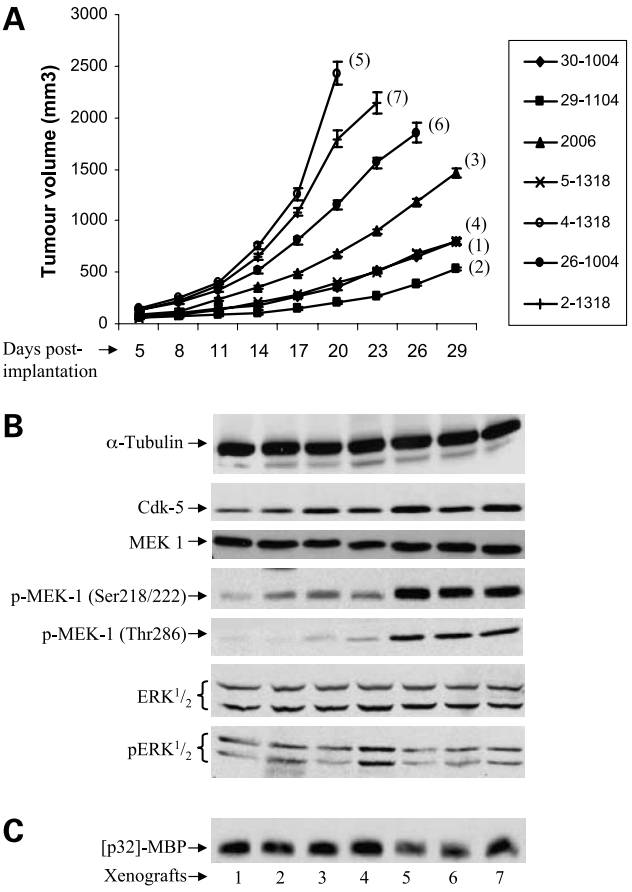

Figure 3. Growth behavior of seven HCC xenografts and their basal levels of MEK1, Cdk-5, ERK1/2, phosphorylated ERK1/2, and phosphorylated MEK1 at $Ser^{218/222}$ and Thr^{286}. The indicated lines of HCC xenografts were established as described in Materials and Methods. **A,** the growth rate of each line of xenografts shown was previously presented (30). **B,** tumors from each line of xenografts were collected and Western blotting was done as described in Materials and Methods. Blots were incubated with the indicated antibodies. **C,** basal MEK kinase activity for each line of xenografts was done as described in Materials and Methods; the [^{32}P]MBP levels were presented. Note that the numbers in parentheses for the curves in **A** correspond to the columns in **B**.

We next examined the association between antitumor activity of AZD6244 and its ability to inhibit the MEK-ERK phosphorylation and activity in 4-1318 xenografts. Tumors were harvested on day 21, 3 h after administration of either AZD6244 or vehicle. As shown in Fig. 6, phosphorylated ERK1/2 (Fig. 6A) and MEK kinase activity (Fig. 6B) in 4-1318 tumors obtained from animals treated with 50 mg/kg AZD6244 was significantly decreased compared with vehicle-treated mice ($P < 0.01$). Similarly, AZD6244 significantly inhibited phosphorylation of ERK1/2 in 2-1318, 5-1318, and 26-1004 (Fig. 6C). No differences were observed for the total ERK1/2 (Fig. 6A and C). As shown in Fig. 6A, the levels of B-Raf and phosphorylated MEK1 at $Ser^{218/222}$ in AZD6244-treated 4-1318 xenografts were also elevated ($P < 0.01$), suggesting that AZD6244 activated a signaling pathway upstream of MEK but inhibited MEK activity. Because the 90-kDa ribosomal S6 kinase (p90RSK) is a target of ERK1/2 (25) and phosphorylation of p90RSK at Ser^{380}, Thr^{359}, and Ser^{363} is important for its activation (35), we wanted to determine if phosphorylation of p90RSK was also inhibited. Figure 6A shows that phosphorylation of p90RSK at Ser^{380} and $Thr^{359/363}$ was significantly reduced ($P < 0.01$) but not completely suppressed by AZD6244. This suggests that, in HCC, phosphorylation of p90RSK is not entirely dependent on ERK1/2 activity, or that only a small amount of ERK1/2 activity is sufficient to phosphorylate quite a lot of p90RSK. The results show that a positive correlation between the antitumor activity of ADZ6244 and its ability to inhibit ERK activity exists.

We have shown that treatment of primary HCC cells with the MEK1/2-specific inhibitor AZD6244 resulted in growth inhibition and apoptosis. We investigated whether these phenomena also occurred *in vivo*. As shown in Fig. 6A, the cleaved 89-kDa PARP fragment was detected in AZD6244-treated xenografts. The cleaved forms of caspase-3 (19 and 17 kDa fragments) and caspase-7 (19 kDa fragment) were also observed in concordance with cleaved PARP (Fig. 6A). Immunohistochemical analysis revealed that the Ki-67 labeling indexes in the vehicle-treated group and 50 mg AZD6244–treated groups were 14.4 ± 3.6% and 4.3 ± 1.8%, respectively. The percentages of cells that stained for cleaved caspase-3 were 0.1 ± 0.1% and 4.5 ± 2.7% for the vehicle-treated group and 50 mg of AZD6244 per kilogram of body weight group, respectively. Similar results were obtained when sections from 2-1318, 26-1004, 29-1104, and 5-1318 xenografts were stained with Ki-67 and cleaved caspase-3 antibodies (data not shown). These results support the view that the reduction in HCC growth and induction of apoptosis by AZD6244 is associated with the inhibition of cell proliferation and caspase-3 activation.

Discussion

Neither the systemic chemotherapy nor hormonal therapy tested has shown an unequivocal benefit in terms of survival in patients with advanced HCC. Thus, there is a significant unmet medical need for the development of effective therapies able to stabilize or slow the progression

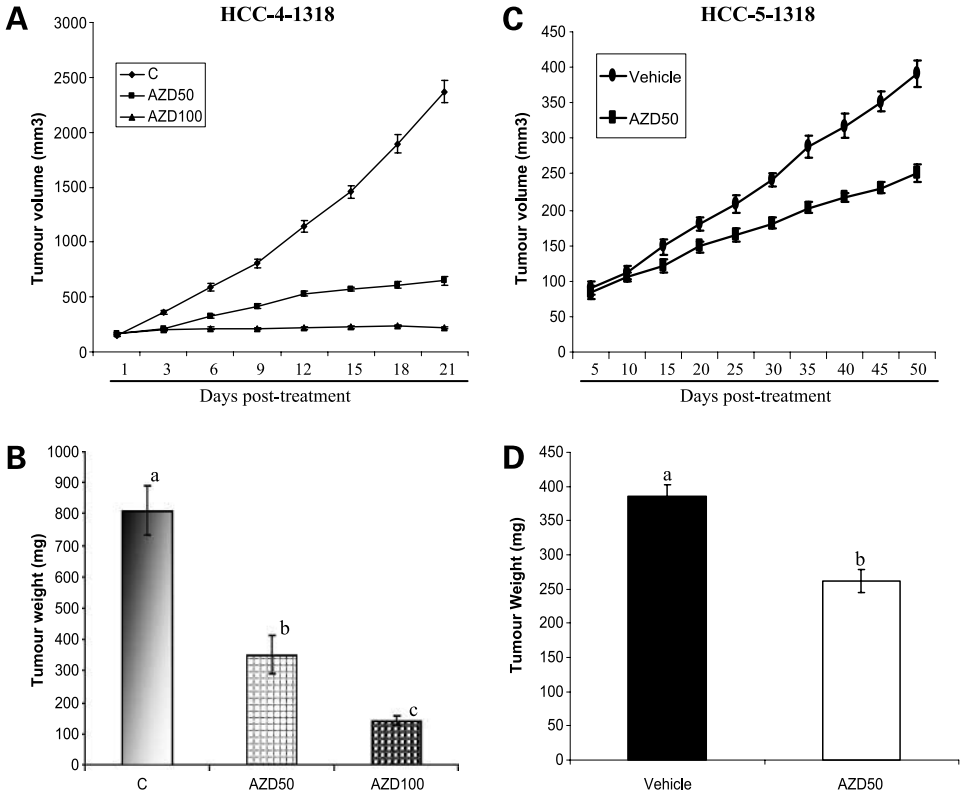

Figure 4. Effects of AZD6244 on growth rate and tumor weight of HCC xenografts. 4-1318 and 5-1318 xenografts were s.c. implanted on the right side of male *SCID* mice as described in Materials and Methods. Mice bearing xenografts were p.o. given twice a day either with vehicle or AZD6244 for 21 d. **A** and **B,** 50 mg (AZD50) and 100 mg (AZD100) AZD6244 per kilogram of body weight were used for 4-1318 xenografts. **C** and **D,** only the 50-mg dose (AZD50) was used for 5-1318. Treatment started on day 7 after tumor cell injection. Tumor growth was measured and calculated as described in Materials and Methods. Tumor volume at a given time for control and AZD6244-treated 4-1318 (**A**) and 5-1318 (**C**) xenografts is plotted. Each data point represents six to eight tumor samples. Tumor weight at sacrifice for control and AZD6244-treated 4-1318 (**B**) and 5-1318 (**D**) xenografts are shown. Columns with different letters were statistically significant ($P < 0.01$) as analyzed by ANOVA. Experiments were repeated at least twice with similar results.

of HCC. The poor efficacy of medical treatment of patients with HCC and the dissatisfaction with such treatment has motivated the development of HCC xenografts to evaluate the efficacy of novel or existing drugs before clinical trials. Through a better understanding of the molecular basis of hepatocarcinogenesis, new preventative and therapeutic modalities are being developed.

In this study, we show that blockage of MEK1/2 activity with AZD6244 results in growth arrest and apoptosis in established HCC *in vivo*. The growth behavior of HCC xenografts is positively correlated with the levels of phosphorylated MEK1 at Ser$^{218/222}$ and Thr^{286}. At a dose of 50 mg/kg, AZD6244 does not cause any apparent harm to the animals, but does suppress tumor growth in a dose-dependent manner. Treatment of primary human liver cancer cells with the MEK inhibitor AZD6244, which inhibits the MEK-ERK pathway activation, leads to a time- and dose-dependent reduction in cell proliferation and viability, implicating the requirement of MEK activity for liver cancer cells to proliferate and survive.

The presence of activated MEK in aggressive HCC xenografts suggests that MEK activation may be linked to the malignant progression of liver cancer. It has been

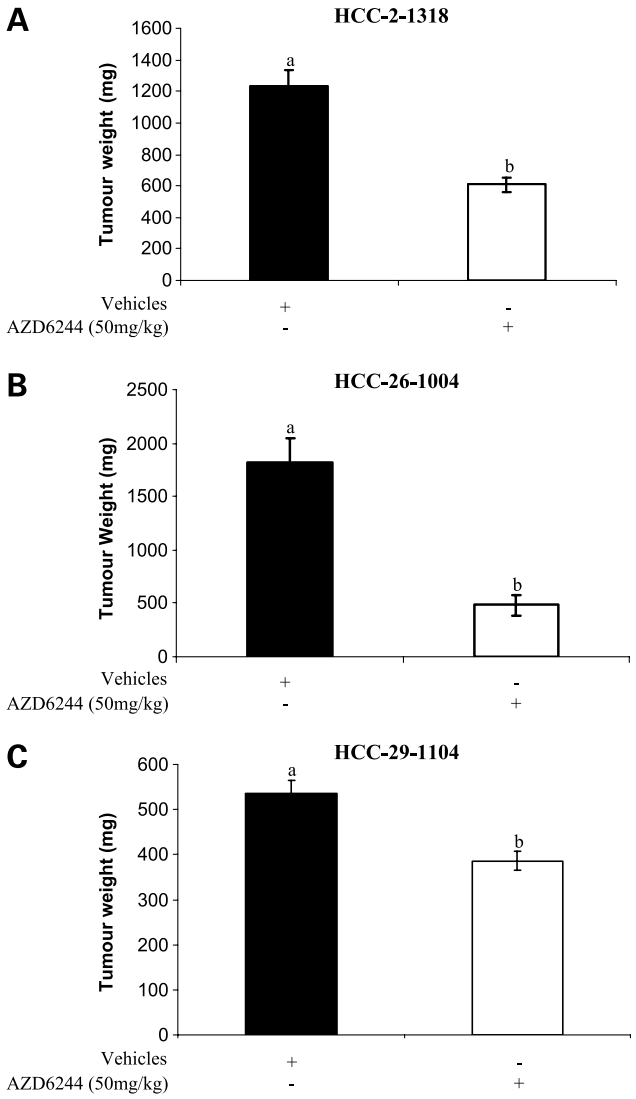

Figure 5. Effects of AZD6244 on tumor weight of 2-1318, 26-1004, and 29-1104 xenografts. Indicated lines of HCC xenografts were implanted as described above. Mice bearing xenografts were p.o. given twice a day either with vehicle or 50 mg/kg of AZD6244 for 21 d. Treatment started on day 7 after tumor cell injection. Tumor growth was measured and calculated as described in Materials and Methods. Tumor weight at sacrifice for control and AZD6244-treated xenografts, 2-1318 (**A**), 26-1004 (**B**), and 29-1104 (**C**). Columns with different letters were statistically significant ($P < 0.01$) as analyzed by ANOVA. Experiments were repeated at least twice with similar results.

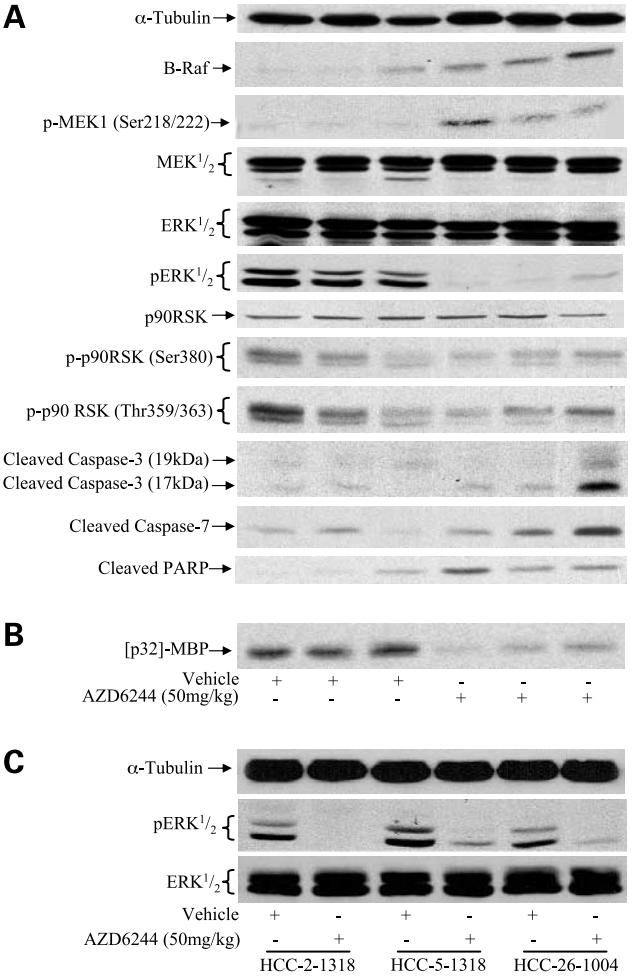

Figure 6. Effects of AZD6244 on the levels of B-Raf; phosphorylation of MEK1, ERK1/2, and p90RSK; and apoptosis in HCC xenografts. Indicated HCC xenografts were implanted as described in Materials and Methods. Mice bearing indicated xenografts were p.o. given, twice daily, with either vehicle or 50 mg AZD6244 per kilogram for 21 d. Lysates from 4-1318, 2-1318, and 5-1318 (**A**), and 26-1004 (**C**) tumors were subjected to Western blot analysis as described in Materials and Methods. Blots were incubated with indicated antibodies. **B,** basal MEK1 kinase activity for vehicle- and AZD6244-treated 4-1318 xenografts was done as described in Materials and Methods, and the [^{32}P]MBP levels are shown. Representative samples. Experiments were repeated at least twice with similar results.

shown that expression of cyclin D1 is controlled by MEK-ERK signaling (36, 37), and expression of activated mitogen-activated protein kinase phosphatase 1, a negative regulator of MEK (38), significantly depresses the ability of these cells to proliferate in response to growth factor stimulation. In the present study, the high levels of phosphorylated MEK observed in fast-growing xenografts may reflect local autocrine/paracrine signaling. Activation of MEK-ERK by autocrine/paracrine growth factors may help the cells survive even in the presence of limited nutrients, and to increase the secretion of angiogenic factors from the tumor cells (39, 40). *In vivo*, these angiogenic factors then stimulate neovascularization, which is essential for the growth, survival, invasion, and metastasis of liver cancer cells. It is possible that the AZD6244-induced apoptosis *in vivo* is also related to the inhibition of neovascularization. It has been reported that PD98059 and U0126, two other MEK inhibitors, are able to impede the growth of Ras-transformed cells in soft agar and to reduce the urokinase secretion controlled by growth factors such as epidermal growth factor, transforming growth factor-α, and fibroblast growth factor in an autocrine manner in the squamous cell carcinoma cell lines UM-SCC-1 and MDA-TV-138 (41). It remains to be determined whether AZD6244 is able to control invasive tumor phenotype of HCC cells. Experiments are under way to investigate this possibility.

In mammalian cells, there are at least two pathways involved in apoptosis. One involves caspase-8, which is recruited by the adapter molecule Fas/APO-1–associated death domain protein to death receptors upon extracellular ligand binding (42, 43). The other involves cytochrome *c* release–dependent activation of caspase-9 through Apaf-1 (44, 45). No changes in either Fas or FasL expression in AZD6244-treated primary HCC cells was observed. We did observe increased cleaved caspase-3, cleaved caspase-7, and cleaved PARP in AZD6244-treated cells. It remains to be determined whether ADZ6244 also causes the release of cytochrome *c*, which is responsible for the activation of both caspase-7 and caspase-3.

In the present study, we did not observe a correlation between phosphorylated MEK1 and ERK1/2. The basal levels of phosphorylated ERK1/2 and MEK kinase activity in fast-growing xenografts are slightly lower than slow-growing ones. Given the role of MEK in ERK phosphorylation, it is interesting to observe that three lines of the HCC xenografts exhibit increased, sustained activation of MEK1 at $Ser^{218/222}$ and Thr^{286} but not ERK1/2. It has been reported that Cdk-5 phosphorylates MEK1 at Thr^{286} and this phosphorylation results in inhibition of MEK1 catalytic activity and the phosphorylation of ERK1/2 (46). It is possible that slightly low levels of MEK kinase activity and phosphorylated ERK1/2 in fast-growing xenografts are due to high basal expression of Cdk-5 that suppresses MEK activity by phosphorylating MEK at Thr^{286}. In the present study, we also observed that B-Raf and phosphorylated MEK1 at $Ser^{218/222}$ and $Ser^{217/221}$ are elevated in AZD6244-treated xenografts and primary cells. These suggest that AZD6244 also activates a signaling pathway upstream of MEK. Because MEK is a target of B-Raf, it is possible that elevation in phosphorylated MEK but not ERK1/2 *in vivo* and *in vitro* following AZD6244 treatment is due to AZD6244-induced up-regulation of B-Raf (Fig. 6A).

Unlike the case with cytotoxic agents, HCC patients responding to treatment with a signal transduction inhibitor such as AZD6244 are likely to share common molecular alterations of the target or pathway, such as Ras or Raf mutations driving activation of the MEK-ERK pathway. The present study shows that the 5-1318 and 29-1104 lines, expressing low levels of phosphorylated MEK1, are relatively less sensitive to AZD6244. This suggests that patients with high levels of activated MEK in their tumors will respond to AZD6244 in a more potent manner than patients who have low levels of activated MEK. Designing clinical trials that accrue patients based on the level of activated MEK in their tumors is therefore a special interest. Analysis of tumor samples for this specific biomarker is important for determining the likely *in vivo* effects of AZD6244 inhibitor. Here, we have shown that AZD6244 inhibits tumor growth when given alone, suggesting that at least some patients may be amenable to single-agent therapy. As for all potential anticancer drugs, inhibitors of the MEK-ERK pathway may not be very effective as individual therapeutic agents because HCC tumors possess more than one genetic defect (15). For maximal therapeutic benefit, it may be necessary to combine AZD6244 with another signal transduction inhibitor or conventional chemotherapeutic drugs such as doxorubicin or 5-fluorouracil. In the meantime, a multitude of other targeted agents have become available that should also tested in combination with MEK inhibitors. The elucidation of the optimal combinations can be expected to unfold over time.

We have shown that treatment of HCC cells with the MEK inhibitor AZD6244 leads to growth inhibition and apoptosis *in vitro*. Using five lines of xenografts, we show that p.o. delivery of AZD6244 causes growth inhibition of HCC xenografts *in vivo* and induces apoptosis in liver cancer cells. Our data implicate important role(s) of the activated MEK-ERK pathway in liver cancer cell proliferation and survival. Therefore, targeted inhibition of MEK activity by AZD6244, or other MEK inhibitors such as PD0325901 (15), may represent a highly valuable alternative approach for the treatment of HCC.

Acknowledgments

We thank Dr. Paul D. Smith (AstraZeneca, Macclesfield, Cheshire, United Kingdom) for the gift of ADZ6244 and the American Journal Experts for reviewing the manuscript before submission.

References

1. Akriviadis EA, Llovet JM, Efremidis SC, et al. Hepatocellular carcinoma. Br J Surg 1998;85:1319–31.

2. Parkin DM, Bray F, Ferlay J, Pisani P. Global cancer statistics, 2002. CA Cancer J Clin 2005;55:74–108.

3. Schafer DF, Sorrell MF. Hepatocellular carcinoma. Lancet 1999;353:1253–7.

4. Ince N, Wands JR. The increasing incidence of hepatocellular carcinoma. N Engl J Med 1999;340:798 – 9.

5. Chedid A, Ryan LM, Dayal Y, Wolf BC, Falkson G. Morphology and other prognostic factors of hepatocellular carcinoma. Arch Pathol Lab Med 1999;123:524 – 8.

6. Okuda K, Ohtsuki T, Obata H, et al. Natural history of hepatocellular carcinoma and prognosis in relation to treatment. Study of 850 patients. Cancer 1985;56:918 – 28.

7. Colombo M. Hepatocellular carcinoma. J Hepatol 1992;15:225 – 36.

8. Lai EC, Fan ST, Lo CM, Chu KM, Liu CL, Wong J. Hepatic resection for hepatocellular carcinoma. An audit of 343 patients. Ann Surg 1995;221: 291 – 8.

9. Takenaka K, Kawahara N, Yamamoto K, et al. Results of 280 liver resections for hepatocellular carcinoma. Arch Surg 1996;131:71 – 6.

10. Huguet CSFaGA. Over-expression of the mitogen-activated protein kinase (MAP kinase). In: L Blumgart, editor. Surgery of the liver and biliary tract. London: Churchill Livingstone; 2000. p. 1365 – 69.

11. Lai EaWJ. Hepatocellular carcinoma: the Asian experience. In: L Blumgart, editor. Surgery of the liver and the biliary tract. London: Churchill Livingstone; 1994. p. 1349 – 63.

12. Chan ES, Chow PK, Tai B, Machin D, Soo K. Neoadjuvant and adjuvant therapy for operable hepatocellular carcinoma. Cochrane Database Syst Rev 2000;2:CD0011991199.

13. Zeng JZ, Wang HY, Chen ZJ, Ullrich A, Wu MC. Molecular cloning and characterization of a novel gene which is highly expressed in hepatocellular carcinoma. Oncogene 2002;21:4932 – 43.

14. Huynh H, Chow PK, Ooi LL, Soo KC. A possible role for insulin-like growth factor-binding protein-3 autocrine/paracrine loops in controlling hepatocellular carcinoma cell proliferation. Cell Growth Differ 2002;13: 115 – 22.

15. Sebolt-Leopold JS, Herrera R. Targeting the mitogen-activated protein kinase cascade to treat cancer. Nat Rev Cancer 2004;4:937 – 47.

16. Hoshino R, Chatani Y, Yamori T, et al. Constitutive activation of the 41-/43-kDa mitogen-activated protein kinase signaling pathway in human tumors. Oncogene 1999;18:813 – 22.

17. Amundadottir LT, Leder P. Signal transduction pathways activated and required for mammary carcinogenesis in response to specific oncogenes. Oncogene 1998;16:737 – 46.

18. Dudley DT, Pang L, Decker SJ, Bridges AJ, Saltiel AR. A synthetic inhibitor of the mitogen-activated protein kinase cascade. Proc Natl Acad Sci U S A 1995;92:7686 – 9.

19. Nguyen DH, Catling AD, Webb DJ, et al. Myosin light chain kinase functions downstream of Ras/ERK to promote migration of urokinase-type plasminogen activator-stimulated cells in an integrin-selective manner. J Cell Biol 1999;146:149 – 64.

20. Liu E, Thant AA, Kikkawa F, et al. The Ras-mitogen-activated protein kinase pathway is critical for the activation of matrix metalloproteinase secretion and the invasiveness in v-crk-transformed 3Y1. Cancer Res 2000;60:2361 – 4.

21. Reddy KB, Krueger JS, Kondapaka SB, Diglio CA. Mitogen-activated protein kinase (MAPK) regulates the expression of progelatinase B (MMP-9) in breast epithelial cells. Int J Cancer 1999;82:268 – 73.

22. Anderson NG, Maller JL, Tonks NK, Sturgill TW. Requirement for integration of signals from two distinct phosphorylation pathways for activation of MAP kinase. Nature 1990;343:651 – 3.

23. Ballif BA, Blenis J. Molecular mechanisms mediating mammalian mitogen-activated protein kinase (MAPK) kinase (MEK)-MAPK cell survival signals. Cell Growth Differ 2001;12:397 – 408.

24. Alessi DR, Cuenda A, Cohen P, Dudley DT, Saltiel AR. PD 098059 is a specific inhibitor of the activation of mitogen-activated protein kinase kinase *in vitro* and *in vivo*. J Biol Chem 1995;270: 27489 – 94.

25. Frodin M, Gammeltoft S. Role and regulation of 90 kDa ribosomal S6 kinase (RSK) in signal transduction. Mol Cell Endocrinol 1999;151: 65 – 77.

26. Huynh HT, Nguyen TT, Chow PK, Tan PH, Soo KC, Tran E. Over-expression of MEK-MAPK in hepatocellular carcinoma: its role in tumor progression and apoptosis. BMC Gastroenterol 2003;3:19.

27. Huynh H, Do PT, Nguyen TH, et al. Extracellular signal-regulated kinase induces cyclin D1 and Cdk-2 expression and phosphorylation of retinoblastoma in hepatocellular carcinoma. Int J Oncol 2004;25:1839 – 47.

28. Lee P, Wallace E, Yeh T, et al. Demonstration of broad *in vivo* anti-tumour activity of ARRY-142886 (AZD6244), a potent and selective MEK inhibitor [abstract]. Array BioPharma 2005.

29. Winkler JD, Lee PA, Wallace E, et al. Anti-tumor activity, pharmacokinetic and pharmacodynamic effects of the MEK inhibitor ARRY-142886 (AZD6244) in a BxPC3 pancreatic tumor xenograft model [abstract]. Array BioPharma 2005.

30. Huynh H, Soo KC, Chow PK, Panasci L, Tran E. Xenografts of human hepatocellular carcinoma: a useful model for testing drugs. Clin Cancer Res 2006;12:4306 – 14.

31. Hung H. Suppression of ps20 expression in the rat uterus by tamoxifen and estrogens. Endocrinology 2005;146:2388 – 96.

32. Nguyen TT, Tran E, Ong CK, et al. Kaempferol-induced growth inhibition and apoptosis in A549 lung cancer cells is mediated by activation of MEK-MAPK. J Cell Physiol 2003;197:110 – 21.

33. Alessi DR, Cohen P, Ashworth A, Cowley S, Leevers SJ, Marshall CJ. Assay and expression of mitogen-activated protein kinase, MAP kinase kinase, and Raf. Methods Enzymol 1995;255:279 – 90.

34. Mikula M, Schreiber M, Husak Z, et al. Embryonic lethality and fetal liver apoptosis in mice lacking the c-raf-1 gene. EMBO J 2001;20: 1952 – 62.

35. Dalby KN, Morrice N, Caudwell FB, Avruch J, Cohen P. Identification of regulatory phosphorylation sites in mitogen-activated protein kinase (MAPK)-activated protein kinase-1a/p90rsk that are inducible by MAPK. J Biol Chem 1998;273:1496 – 505.

36. Cheng M, Sexl V, Sherr CJ, Roussel MF. Assembly of cyclin D-dependent kinase and titration of p27Kip1 regulated by mitogen-activated protein kinase kinase (MEK1). Proc Natl Acad Sci U S A 1998; 95:1091 – 6.

37. Lavoie JN, L'Allemain G, Brunet A, Muller R, Pouyssegur J. Cyclin D1 expression is regulated positively by the p42/p44MAPK and negatively by the p38/HOGMAPK pathway. J Biol Chem 1996;271:20608 – 16.

38. Brondello JM, McKenzie FR, Sun H, Tonks NK, Pouyssegur J. Constitutive MAP kinase phosphatase (MKP-1) expression blocks G1 specific gene transcription and S-phase entry in fibroblasts. Oncogene 1995;10:1895 – 904.

39. Petit AM, Rak J, Hung MC, et al. Neutralizing antibodies against epidermal growth factor and ErbB-2/neu receptor tyrosine kinases down-regulate vascular endothelial growth factor production by tumor cells *in vitro* and *in vivo*: angiogenic implications for signal transduction therapy of solid tumors. Am J Pathol 1997;151:1523 – 30.

40. Eliceiri BP, Klemke R, Stromblad S, Cheresh DA. Integrin $\alpha_v\beta_3$ requirement for sustained mitogen-activated protein kinase activity during angiogenesis. J Cell Biol 1998;140:1255 – 63.

41. Simon C, Juarez J, Nicolson GL, Boyd D. Effect of PD 098059, a specific inhibitor of mitogen-activated protein kinase kinase, on urokinase expression and *in vitro* invasion. Cancer Res 1996;56:5369 – 74.

42. Muzio M, Stockwell BR, Stennicke HR, Salvesen GS, Dixit VM. An induced proximity model for caspase-8 activation. J Biol Chem 1998;273: 2926 – 30.

43. Cryns V, Yuan J. Proteases to die for. Genes Dev 1998;12: 1551 – 70.

44. Cai J, Yang J, Jones DP. Mitochondrial control of apoptosis: the role of cytochrome *c*. Biochim Biophys Acta 1998;1366:139 – 49.

45. Zou H, Li Y, Liu X, Wang X. An APAF-1.cytochrome *c* multimeric complex is a functional apoptosome that activates procaspase-9. J Biol Chem 1999;274:11549 – 56.

46. Sharma P, Veeranna SP, Sharma M, et al. Phosphorylation of MEK1 by cdk5/p35 down-regulates the mitogen-activated protein kinase pathway. J Biol Chem 2002;277:528 – 34.

Molecular Cancer Therapeutics

Targeted inhibition of the extracellular signal-regulated kinase kinase pathway with AZD6244 (ARRY-142886) in the treatment of hepatocellular carcinoma

Hung Huynh, Khee Chee Soo, Pierce K.H. Chow, et al.

Mol Cancer Ther 2007;6:138-146.